

Virus Antibody Dynamics in Primary and Secondary Dengue Infections

Tanvi P. Gujarati · G. Ambika

Received: date / Accepted: date

Abstract Dengue viral infections show unique infection patterns arising from its four serotypes, (DENV-1,2,3,4). Its effects range from simple fever in primary infections to potentially fatal secondary infections. We analytically and numerically analyse the humoral response of a host to primary and secondary dengue infection using micro-epidemic models. The models incorporate time delays, antibody dependent enhancement (ADE), a dynamic switch and a correlation factor between different DENV serotypes. We find that the viral load goes down to undetectable levels within 7-14 days of infection in both cases. Stability analysis of the model shows interesting dependence on the time delays. We demonstrate the existence of a critical value for the immune response parameter, beyond which re-infection with a homologous serotype is not detectable. For secondary infections of a different serotype, the homologous antibody production is enhanced due to the influence of heterologous antibodies and is also controlled by the correlation factor, a measure of similarities between the different DENV serotypes involved, introduced in this work. We successfully replicate clinically observed humoral responses for primary and secondary infections.

Keywords Humoral immune response · Antibody dependent enhancement · Correlation factor among serotypes · Time delay · Stability analysis

Mathematics Subject Classification (2010) 37N25 · 34A34 · 92B05 · 92C60

1 Introduction

Dengue, a vector-borne infectious disease caused by the dengue virus (DENV), is one of the gravest and most difficult to understand diseases infecting humans. The biological mechanisms and dynamical processes involved during this infection therefore demand a serious study, which is especially relevant from the point of view of a complex non-linear biological model with varied and rich dynamics. Dengue is transmitted to humans

Tanvi P. Gujarati
Indian Institute of Science Education and Research, Tvm, Thiruvananthapuram-695016, Kerala, India,
E-mail: tanvi@iisertvm.ac.in

G. Ambika
Indian Institute of Science Education and Research, Pune, Pune-411021, Maharashtra, India,
E-mail: g.ambika@iiserpune.ac.in

through the bite of infected *Aedes aegypti* and *A. albopictus* mosquitoes. According to WHO estimates, 50 to 100 million infections occur each year leading to 500,000 hospitalizations and 20,000 deaths (<http://www.who.int/mediacentre/factsheets/fs117/en>). Until recently dengue was considered to be a disease of the tropics, but now it has spread its domain of infection to temperate regions as well, primarily boosted by global warming (<http://www.sciencedaily.com/releases/1998/03/980310081157.html>). It is understood that four closely related serotypes of DENV exist viz. DENV-1, DENV-2, DENV-3 and DENV-4 [1,2] and these four serotypes cause infections of varying severity in humans. The infected individual usually suffers from acute febrile illness called Dengue Fever (DF) which is cleared by a complex immune response in a short time of approximately 7 days after onset of fever. There are more severe manifestations of this disease like dengue hemorrhagic fever (DHF) and dengue shock syndrome (DSS). Often without immediate and necessary proper treatment DHF/DSS can be fatal [3,4,5]. We note that there is no specific drug or vaccine yet developed to prevent its infection.

The epidemiology of dengue in varied populations have been studied previously using improved or extended versions of the basic SIR model [6,7,8,9,10,11,12,13]. Here we present a mathematical model on a cellular scale incorporating time delay in immune response which is very relevant and important in this context. A few such models describing the cell-virus interaction dynamics have been studied in other contexts like HIV or hepatitis [14,15]. However, micro-epidemiological studies reported in the context of DENV are very few, one such study reported recently involves T-cell immune response. [16].

In this work we propose a within-host dynamical model that involves humoral or antibody-antigen immune response which is known to be more important for dengue virus - host interactions. We also introduce intra cellular time delays that come from the various steps involved during antibody production [17,18]. Our study indicates how the antibodies and their interactions play a decisive role in the dynamics. We carry out a detailed stability analysis followed by numerical analysis to identify the relevant range of parameters that correspond best with the observed facts. We find that there exists a critical value for the immune response parameter above which the disease free state is always stable. However large time delay in antibody production can upset this and lead to oscillatory nature of the virus counts.

We extend the primary infection model to a 6-dimensional secondary infection model with heterologous and homologous antibodies. To the best of our knowledge, it is the first attempt at modelling the secondary dengue infection on a micro-epidemic scale, with novel features like time delays, correlation factor between the viral serotypes and a dynamic switch. The correlation factor is introduced to bring in the relatedness in the different DENV serotypes into the dynamics, which is very important in the context of secondary infection. The dynamical switch in our model toggles between different values based on the antibody concentrations present from the primary infection. With these additional parameters, our model can account for Antibody Dependent Enhancement of virus as well as the increased antibody counts observed clinically during secondary dengue infection. Further modifications of the models by including effects of vaccination may help in realising precautionary mechanisms to combat dengue, which will be a major breakthrough since no effective vaccine exists as of now against dengue.

Before proceeding further, it is imperative to consider what DENV does once introduced into the human body by an infected mosquito. After the entry of virions into the body, it is understood that the virions infect macrophages, monocytes, dendritic cells, mast cells and hepatocytes [19,20,21,22]. Once inside the target cells, these virions start multiplying in the infected cells and burst out of them in large numbers, thus aggravating the infection.

Virions incite a counter-reaction in the form of an immune response to curb this infection. There exist different complex mechanisms which form the immune response, out of which the humoral immune response is of utmost relevance as far as dengue is concerned [17, 18, 2]. On coming in contact with the antigens present on the virus particles, the B-cells of the body start the process of producing antibodies which are proteins made to complement the antigens and which then neutralise the virus particles, making them non-infectious. These virus-antibody aggregates are then chemically degraded and destroyed in the macrophages (note that macrophages are also DENV targets). The external manifestations of this whole process is what we generally see as an acute febrile illness that gets cured within 7-14 days even in the absence of medication. If a person is introduced to DENV of any serotype for the first time, it is termed as primary infection. It is observed that infection with a serotype provides life-long immunity against that serotype, i.e. recurrence of dengue infection with the same serotype is not observed. This is because the ‘memory’ of the previous infection suppresses the spread of virions without much delay.

If an individual who has already undergone primary infection is again exposed to DENV of a different serotype then it is called secondary infection. It is generally observed that complicated and fatal conditions of DSS/DHF occur in patients suffering from secondary infection. What makes primary infection easy for the body to deal with and secondary infection so severe? To answer this question we must look at what happens when a different DENV serotype enters the body that is already prepared to tackle previous DENV serotype. The new DENV serotype is structurally similar to the old one, hence it leads to production of antibodies that complement the old serotype (i.e. cross immunity) along with new antibodies that are made to combat the new serotype. Thus, there are mainly two relevant antibodies now, one from the old infection which are heterologous to the new serotype and the new homologous antibodies from the present infection. Both these antibodies have the capacity to bind to virions and neutralise them. Once neutralised the antibody-virus complex is taken to the macrophages. This time though, on entering the macrophage, the heterologous antibodies are released from the virus due to their low affinity for this new serotype. This makes a fraction of the virus particles bare and ready for infecting the macrophage. Thus the antibodies produced against the new serotype protects as well as carries the virus to their targets depending on the affinity between the antigen and antibody. This process is termed as the Antibody Dependent Enhancement (ADE) of infection. Clinically it is observed that during the secondary infection the viral counts are higher than that of the primary infection but the virus clears from the body in about the same time. The striking feature of secondary infections is a very high concentration of antibodies in the bodies of patients. In fact, it is this high load of antibodies which further leads to severe conditions described by DSS/DHF. Therefore, it is the nature of the immune response that plays a critical role in the study of dengue [23, 2].

In this paper we present the mathematical models describing primary and secondary dengue infections based on the intracellular mechanisms described above and analyse them mathematically and computationally. The paper proceeds by describing the primary model in section 2, its analytical treatment in section 3, secondary infection model in section 4, its numerical analysis in section 5 and conclusions in section 6.

2 Model describing primary dengue infection

We present the mathematical model describing the primary infection as a 5-D model that takes into consideration the viral dynamics and humoral immune response as described in

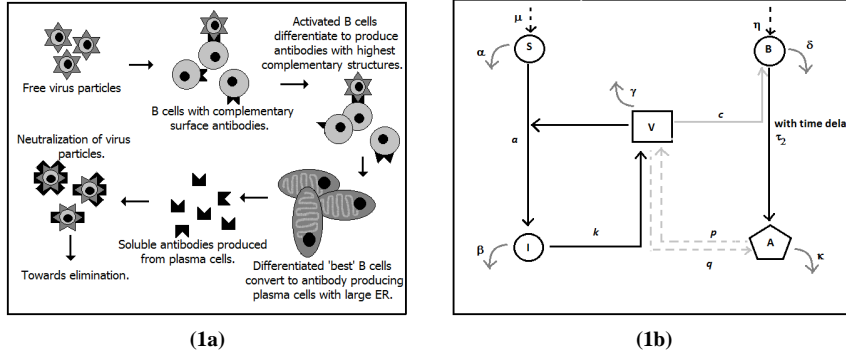


Fig. 1 Humoral immune response in primary dengue infection. 1a. Cartoon representation of virus-antibody interactions. 1b. Schematic of the mathematical model. Dashed black arrows stand for intrinsic growth rate. Solid black arrows depict conversion and infection. Solid straight grey arrow shows activation rate. Curved grey arrows show intrinsic death rates and dashed grey arrows show elimination rates.

Table 1 Description of the parameters used in the model.

Parameter Symbols	Parameter Description
μ	Production rate of healthy cells
α	Death rate of healthy cells
a	Rate at which healthy cells are converted to infected cells
β	Death rate of infected cells
k	Burst rate of virus particles
γ	Rate at which virus particles degrade
p	Rate at which virus particles are neutralised by antibodies
η	Production rate of B-lymphocytes
δ	Death rate of B cells
c	Rate at which B cells are stimulated by virus particles
f	Rate at which stimulated B cells (Plasma cells) produce antibodies
q	Rate at which virus antibody complexes are destroyed.
κ	Rate at which free antibodies degrade.

the introduction. It is built on the basic 3-D model i.e. healthy cells, infected cells and virus particles proposed by May and Nowak [14]. The pictorial representation of the B-cell dependent humoral response is given in Figure (1a) and a schematic representation of the model described below is shown in Figure(1b) The equations describing the model are given by:

$$\begin{aligned}
 \dot{S} &= \mu - \alpha S - aSV \\
 \dot{I} &= aSV - \beta I \\
 \dot{V} &= kI - \gamma V - pAV \\
 \dot{B} &= \eta - \delta B + cBV \\
 \dot{A} &= fH(t - \tau_1)B(t - \tau_2) - qAV - \kappa A
 \end{aligned} \tag{1}$$

where the relevant variables are: S-healthy cells (e.g. Human monocytes/ macrophages), I- infected cells, V-Dengue virus particles, B- B lymphocytes and A-neutralizing antibodies. The description of the parameters controlling the dynamics are given in table.1.

The concept of Heaviside step function, H , and delay in antibody production is similar to the ones used earlier in immune response models [24,25]. However our model includes two different time delays τ_1 and τ_2 . The time delay τ_1 , introduced through the Heaviside step function, is the time period that is required for the first production of antibodies after the virus and B-lymphocytes interact. This delay is biologically significant since production of antibodies after the virions have interacted with the B-lymphocytes is a complex process involving multiple steps. The B-cells have to undergo differentiations before they can be transformed into the plasma cells capable of producing antibodies[26]. Thus the Heaviside step function $H(t)$ is defined as,

$$\begin{aligned} H(t - \tau_1) &= 0 & \text{for } t < \tau_1 \\ H(t - \tau_1) &= 1 & \text{for } t \geq \tau_1 \end{aligned} \quad (2)$$

The other time delay τ_2 , introduced in our model, takes into consideration the time required to produce antibodies from plasma cells (which are modified B-cells). At any time t , the model will consider the plasma cell (same variable as B-cells in our model) concentration present at time $(t - \tau_2)$. From the descriptions of both the time delays, it follows that $\tau_1 > \tau_2$. For this model the reproduction ratio, R_0 , calculated by using the next generation method [27] is:

$$R_0 = \frac{a\mu k}{\alpha\beta\gamma} \quad (3)$$

For certain conditions ($c = 0, f = 0, A(0) = 0$), the present model gets decoupled with respect to the variable B and it reduces to the original model by Nowak and May [14] which is independent of the time delay τ_2 . Detailed analysis of other mathematical models describing virus dynamics have been discussed by Leenheer and Smith [28]. The detailed stability analysis of steady states based on model described by equations (1) is given in the next section.

3 Analysis of equilibrium states and their stability

We now look at the stability analysis of equilibrium states of the dynamics described by the equations (1)[29]. The equilibrium values thus obtained are (denoted with $'^*'$) :

$$S^* = \frac{\mu}{(\alpha + aV^*)} \quad (4a)$$

$$I^* = \frac{aS^*V^*}{\beta} \quad (4b)$$

$$B^* = \frac{\eta}{(\delta - cV^*)} \quad (4c)$$

$$A^* = \frac{fB^*}{(qV^* + \kappa)} \quad (4d)$$

and

$$V^*(p_3V^{*3} + p_2V^{*2} + p_1V^* + p_0) = 0 \quad (5)$$

where

$$p_3 = qca\gamma \quad (6a)$$

$$p_2 = [a\gamma(c\kappa - q\delta) - qc\alpha\gamma(R_0 - 1)] \quad (6b)$$

$$p_1 = [\alpha\gamma(q\delta - \kappa c)(R_0 - 1) - \kappa\gamma\delta a - apf\eta] \quad (6c)$$

$$p_0 = \alpha[\kappa\delta\gamma(R_0 - 1) - fp\eta] \quad (6d)$$

We note that the disease free equilibrium corresponding to the state $V^* = 0$ exists under all conditions and the value of V^* must be less than $\frac{\delta}{c}$ for it to be biologically significant. To make mathematical analysis convenient we consider:

$$\frac{\alpha}{a} = \frac{\delta}{c} = \frac{\kappa}{q} = C \quad (7a)$$

$$D = \frac{fp\eta}{qc\gamma} \quad (7b)$$

Using these in equations (6) we get

$$p_3 = 1 \quad (8a)$$

$$p_2 = -C[R_0 - 1] \quad (8b)$$

$$p_1 = -[C^2 + D] \quad (8c)$$

$$p_0 = C[C^2(R_0 - 1) - D] \quad (8d)$$

The equation (5) can now be solved analytically to get the following roots:

$$V^* = 0 \quad (9a)$$

$$V^* = -C \quad (9b)$$

$$V^* = \frac{C}{2}[R_0 \pm \sqrt{(R_0 - 2)^2 + 4\frac{D}{C^2}}] \quad (9c)$$

We already know that the root $V^* = 0$ exists under all conditions. The second root i.e. $V^* = -C$ is biologically irrelevant since it is negative. Further mathematical analysis shows that only the root given by

$V^* = V_1 = \frac{C}{2}[R_0 - \sqrt{(R_0 - 2)^2 + 4\frac{D}{C^2}}]$ is less than $\frac{\delta}{c}$. Note that this root exists only when $R_0 > 1$ and $f < (R_0 - 1)\frac{\kappa\delta\gamma}{p\eta} = f_c$. Here f_c is the critical value of f for a given R_0 . The equilibrium values of the other variables can then be derived by using equations (4).

To study the stability of the equilibrium state, we linearise the system about the equilibrium points and solve the corresponding Jacobian matrix for eigenvalues. If all the real parts of the eigenvalues obtained by solving the characteristic equation are negative it implies that the system is stable in that equilibrium state. By linearising the system about V^* , we get the Jacobian matrix given below following the procedure given in [30]

$$J = \begin{bmatrix} -(\alpha + aV^*) & 0 & -aS^* & 0 & 0 \\ aV^* & -\beta & aS^* & 0 & 0 \\ 0 & k & -(\gamma + pA^*) & 0 & -pV^* \\ 0 & 0 & cB^* & -(\delta - cV^*) & 0 \\ 0 & 0 & -qA^* & fe^{-\lambda\tau_2} & -(\kappa + qV^*) \end{bmatrix} \quad (10)$$

Here λ stands for the eigenvalues of the Jacobian matrix J given above. On substituting the values of S^* , B^* and A^* in terms of V^* , we get the modified Jacobian which is given in appendix A. A generalised characteristic equation for the Jacobian can be written as (details given in appendix A)

$$\begin{aligned} G(\lambda) &= \lambda^5 + G_4\lambda^4 + G_3\lambda^3 + G_2\lambda^2 + G_1\lambda + G_0 \\ &\quad + H_2e^{-\lambda\tau_2}\lambda^2 + H_1e^{-\lambda\tau_2}\lambda + H_0e^{-\lambda\tau_2} \\ &= 0 \end{aligned} \quad (11)$$

It is clear that the presence of time delay in the dynamics makes the characteristic equation transcendental. Hence the derivation of stability criteria is not straight forward. However we can continue with the analysis by assuming that the eigenvalues are a continuous function of the time delay τ_2 . For $\tau_2 = 0$, the above characteristic equation has negative real parts of the eigenvalues when it satisfies the Routh-Hurwitz criterion for a 5th order polynomial [31]. As we now start increasing the value of τ_2 from 0, the eigenvalues will start changing correspondingly. If the system is stable for $\tau_2 = 0$, i.e. $\lambda(\tau_2) = \varepsilon(\tau_2) + i\omega(\tau_2)$, $\varepsilon(\tau_2) < 0$ and $\omega > 0$ and $\omega \in \mathbb{R}$, then, on increasing τ_2 the system will become unstable when $\varepsilon(\tau_2) > 0$. For this to happen the real part of the eigenvalue must cross zero, i.e. for a particular value of τ_2 say τ_2^0 we must get $\lambda(\tau_2^0) = i\omega_0$. If there is no such value of τ_2 for which the eigenvalue is purely imaginary, the real part of eigenvalues will not change its sign, i.e. system will remain stable for all values of τ_2 if it was stable for $\tau_2 = 0$ [30]. Hence we start our analysis by considering the stable regions for $\tau_2 = 0$ and then continue to find out the regions where change in stability occurs when τ_2 is non-zero.

For $\tau_2 = 0$, the characteristic equation (11) becomes:

$$G(\lambda) = \lambda^5 + G_4\lambda^4 + G_3\lambda^3 + (G_2 + H_2)\lambda^2 + (G_1 + H_1)\lambda + (G_0 + H_0) = 0 \quad (12)$$

According to the Routh-Hurwitz stability criterion for 5th order polynomial we get the following conditions for the stability of the system:

$$\begin{aligned} G_4 &> 0 \\ G_4G_3 - (G_2 + H_2) &> 0 \\ G_4G_3(G_2 + H_2) + G_4(G_0 + H_0) - (G_2 + H_2)^2 - G_4^2(G_1 + H_1) &> 0 \\ (G_1 + H_1)(G_4G_3(G_2 + H_2) + G_4(G_0 + H_0) - (G_2 + H_2)^2 - G_4^2(G_1 + H_1)) \\ - (G_0 + H_0)(G_4G_3^2 + (G_0 + H_0) - G_4(G_1 + H_1) - (G_2 + H_2)G_3) &> 0 \\ (G_0 + H_0) &> 0 \end{aligned} \quad (13)$$

We consider the two parameters, k , the burst rate of virus(k is directly proportional to the reproduction ratio R_0) and f , the production rate of antibodies as the relevant parameters controlling the dynamics and identify regions of stability in the parameter plane f - k . This is done using the maximum value of the real parts of eigenvalues calculated from the characteristic equation (12) as index and is shown in Figure (2). In this plot, we have considered $V^* \neq 0$ root in the region where it exists and $V^* = 0$ root in the other regions. As shown later in section 3.1, $V^* = 0$ root in the region where $V^* \neq 0$ root also exists is unstable, not depicted in this figure. The values of other parameters used are $\mu=10$, $\alpha=0.05$, $a=0.001$, $\beta=0.5$, $\kappa=0.05$, $\gamma=0.5$, $p=0.001$, $\eta=10$, $\delta=0.05$, $c=0.001$, $q=0.001$, $\tau_1=3$ days. The time se-

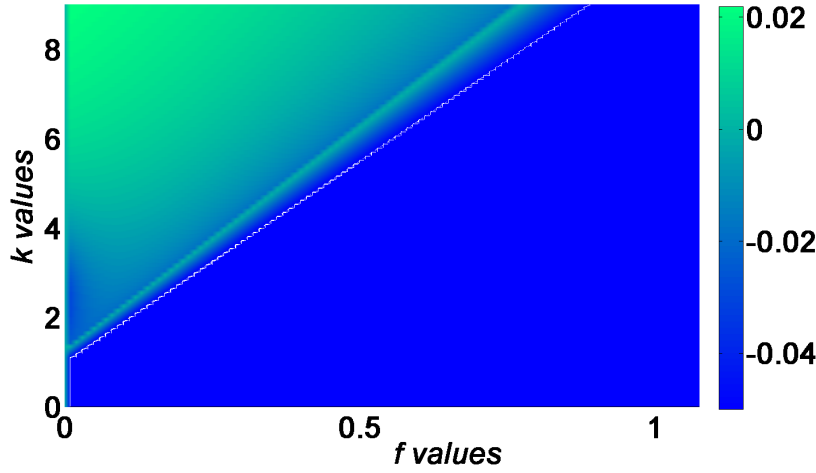


Fig. 2 The parameter plane f - k , indicating stability regions as indexed by the maximum of the real parts of eigenvalues obtained from the characteristic equation (12). Blue(black) end of the spectrum denotes negative values and hence implies that the system is in stable equilibrium in those regions. Similarly the green(grey) end of the spectrum denotes positive values, implying that the system is unstable in those regions. The numerical values of the parameters used are: $\mu=10$, $\alpha=0.05$, $a=0.001$, $\beta=0.5$, $\kappa=0.05$, $\gamma=0.5$, $p=0.001$, $\eta=10$, $\delta=0.05$, $c=0.001$, $q=0.001$, $\tau_1=3$ days.

ries of virus particles corresponding to typical regions in the parameter plane showing different asymptotic dynamics are obtained by direct numerical solution of the model equations and are shown in Figures (3). We find for $f = 0.01$ and $k = 2$ from the stable region in (2), the eigenvalues when $\tau_2 = 0$ are -1.057 , $-0.029 + i 0.066$, $-0.029 - i 0.066$, -0.073 and -0.036 . Hence the equilibrium point is stable. The corresponding time series shows that the virus count goes to a steady non zero value. For $f = 0.1$ and $k = 5$ from the unstable region, the eigenvalues when $\tau_2 = 0$ are -1.724 , $0.0031 + i 0.0850$, $0.0031 - i 0.0850$, -0.089 and -0.083 . Corresponding to this we see oscillatory behaviour for virus count. Similarly, $f = 1$ and $k = 2$ corresponds to the stable region for $V^* = 0$. The corresponding time series for the virus particles tend to zero asymptotically.

Now that the conditions under which the equilibrium point is stable for $\tau_2 = 0$ is analysed, we proceed to get the conditions under which it will remain stable for all values of τ_2 , i.e. conditions under which $\lambda = i\omega$ is not possible. On substituting $\lambda = i\omega$ in the characteristic equation (11) we get;

$$\begin{aligned} G(i\omega) = & i\omega^5 + G_4\omega^4 - iG_3\omega^3 - G_2\omega^2 + iG_1\omega + G_0 - H_2\omega^2(\cos(\omega\tau_2) - i\sin(\omega\tau_2)) \\ & + iH_1\omega(\cos(\omega\tau_2) - i\sin(\omega\tau_2)) + H_0(\cos(\omega\tau_2) - i\sin(\omega\tau_2)) = 0 \end{aligned} \quad (14)$$

On equating the real and imaginary parts of the above equation to zero we get:

$$G_4\omega^4 - G_2\omega^2 + G_0 = (H_2\omega^2 - H_0)\cos(\omega\tau_2) - H_1\omega\sin(\omega\tau_2) \quad (15)$$

$$\omega^5 - G_3\omega^3 + G_1\omega = -(H_2\omega^2 - H_0)\sin(\omega\tau_2) - H_1\omega\cos(\omega\tau_2) \quad (16)$$

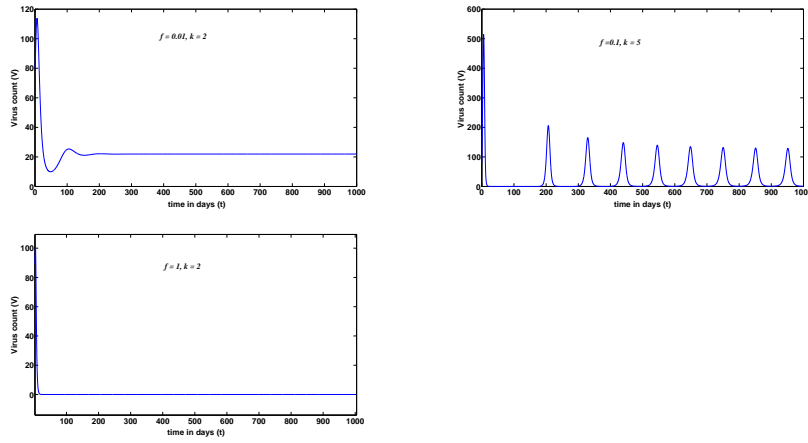


Fig. 3 Asymptotic dynamics of virus count for specific chosen values of the parameters f and k . For $f = 0.01$ and $k = 2$ from the stable region in (2), time series for the virus particles settles to non zero value. For $f = 0.1$ and $k = 5$ from the unstable region the virus particles show oscillatory behaviour. For $f = 1$ and $k = 2$ corresponds to the stable region with $V^* = 0$. The corresponding time series for the virus particles tend to zero asymptotically.

On squaring and adding both sides of equations (15) and (16) we get

$$W(w) = \omega^{10} + (G_4^2 - 2G_3)\omega^8 + (G_3^2 - 2G_4G_2 + 2G_1)\omega^6 + (G_2^2 - H_2^2 + 2(G_4G_0 - G_1G_3))\omega^4 + (G_1^2 - H_1^2 + 2(H_0H_2 - G_0G_2))\omega^2 + (G_0^2 - H_0^2) = 0 \quad (17)$$

Let ω^2 be t in equation (17) and let:

$$\begin{aligned} T_4 &= (G_4^2 - 2G_3) \\ T_3 &= (G_3^2 - 2G_4G_2 + 2G_1) \\ T_2 &= (G_2^2 - H_2^2 + 2(G_4G_0 - G_1G_3)) \\ T_1 &= (G_1^2 - H_1^2 + 2(H_0H_2 - G_0G_2)) \\ T_0 &= (G_0^2 - H_0^2) \end{aligned} \quad (18)$$

Then equation (17) is

$$T(t) = t^5 + T_4t^4 + T_3t^3 + T_2t^2 + T_1t + T_0 = 0 \quad (19)$$

For the stability of the system to remain unchanged we need the ω^2 values obtained from equation (17) to have negative real values. The above equation (19) has at least one real root. Also, we can guarantee that the real parts of the roots of equation (19) are negative when the Routh-Hurwitz criterion for the 5th order polynomial is satisfied by the coefficients

of $T(t)$ i.e.

$$\begin{aligned}
 &T_4 > 0 \\
 &T_4 T_3 - T_2 > 0 \\
 &T_4 T_3 T_2 + T_4 T_0 - T_2^2 - T_4^2 T_1 > 0 \\
 &T_1 (T_4 T_3 T_2 + T_4 T_0 - T_2^2 - T_4^2 T_1) \\
 &\quad - T_0 (T_4 T_3^2 + T_0 - T_4 T_1 - T_2 T_3) > 0 \\
 &T_0 > 0
 \end{aligned} \tag{20}$$

Thus, a point of stability for $\tau_2 = 0$ will not change its stability if it falls in the region defined by the set of equation (20) mentioned above. We once again consider the parameter plane f - k in Figure (4) where light blue regions correspond to values that satisfy the conditions given in equations (20). Here the stable equilibrium points remain stable for nonzero τ_2 . The blue region denotes the regions which change their stability. The yellow regions are the regions which do not have a fixed point solution for $\tau_2 = 0$ and hence are not considered in this analysis. We know that the actual biological processes considered here occur with

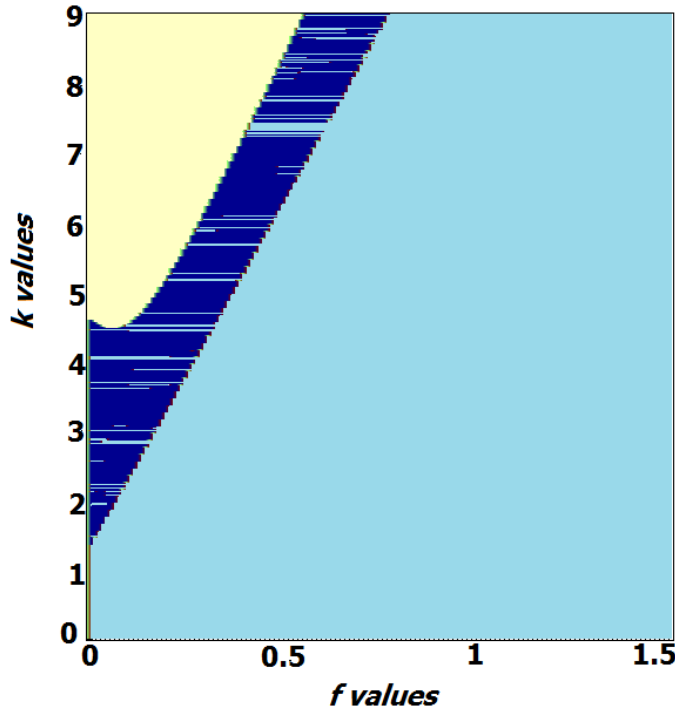


Fig. 4 The parameter plane f - k , indicating regions where change in stability of equilibrium points occurs as τ_2 is increased to nonzero values. Light blue(grey) regions correspond to parameter values for which the stability of the equilibrium points remains the same. Blue(black) regions indicate change in stability while yellow(white) regions are unstable regions for $\tau_2 = 0$.

some inherent non-zero value of time delay. Our analysis indicates that steady states that are stable for $\tau_2 = 0$, can become unstable for a finite time delay τ_2 and the method described here will be useful to analyse the stability for this case.

We now consider an alternate way of analysing stability for nonzero time delay i.e. graphical way of finding dependence of stability on time delay by analysing equation (11) geometrically for $\lambda = i\omega$. We write equation (11) as shown below:

$$e^{-i\omega\tau_2} = \frac{((G_4\omega^4 - G_2\omega^2 + G_0) + i(\omega^5 - G_3\omega^3 + G_1\omega))}{((H_2\omega^2 - H_0) - iH_1\omega)} \quad (21)$$

The left hand side of the equation (21) defines a unit circle on the Argand plane. The right hand side is called the ratio curve. If the ratio curve intersects the unit circle there is a change of stability. By plotting the real and imaginary parts of both sides of equation (21) simultaneously we can check for the change in stability of the equilibrium point. The point of intersection, if any, is given by equation (22) which is derived from equation (21)

$$\tau_2^p = \pm \frac{1}{\omega_0} \arccos \frac{[(H_2\omega_0^2 - H_0)(G_4\omega_0^4 - G_2\omega_0^2 + G_0) - H_1\omega_0(\omega_0^5 - G_3\omega_0^3 + G_1\omega_0)]}{[(H_0 - H_2\omega_0^2)^2 + \omega_0^2 H_1^2]} + \frac{2p\pi}{\omega_0}, \quad p = 0, 1, 2.. \quad (22)$$

We illustrate this analysis by taking the following specific cases:

Case1: For $f = 0.01$ and $k = 2$, which is a point of stable equilibrium for $\tau_2 = 0$, the plots of the unit circle and ratio curve are shown in Figure (5a). As the curves do not intersect, the equilibrium point will be stable for all τ_2 values. The time series for virus particles with $\tau_2 \neq 0$ is shown in Figure (5b)

Case2: For $f = 0.1$ and $k = 3.5$, which was a steady state for $\tau_2 = 0$, the plots of the unit circle and ratio curve intersect each other as shown in Figure (6a). Thus, the equilibrium point changes its stability for the values of τ_2 given by equation (22). Numerically this value turns out to be 8.56 days. The time series for the virus particles before and after this τ_2 value is shown in Figure (6b). We see that the solution is stable for $\tau_2 < 8.56$ and becomes oscillatory for $\tau_2 > 8.56$ days.

The analysis mentioned so far is applicable to the steady states only and does not therefore include the unstable regions shown in Figure(2). Hence for understanding the nature of the dynamics in this region, we numerically analyse the system in equation(1) using 4th order Runge Kutta algorithm and find that the dynamic state corresponding to that region is oscillatory. Thus the oscillatory nature of the state which was observed for $\tau_2 = 0$ persists for $\tau_2 \neq 0$. As a particular case we show the time series for virus count with $\tau_2 \neq 0$ for $f = 0.1$ and $k = 5$ in Figure (7). The corresponding time series for $\tau_2 = 0$ is shown in Figure (3). It is clear that as delay increases, the amplitude of the oscillations increases.

3.1 Disease free equilibrium state

As a special case we look at the stability conditions for $V^* = 0$, the disease free equilibrium state, that is the most interesting case for study. The characteristic equation in this case is given as:

$$G(\lambda) = (\alpha + \lambda)(\kappa + \lambda)(\delta + \lambda)(\lambda^2 + \lambda(\gamma(1 + \frac{fp\eta}{\delta\gamma\kappa}) + \beta) + \beta\gamma(1 + \frac{fp\eta}{\delta\gamma\kappa} - R_0)) \quad (23)$$

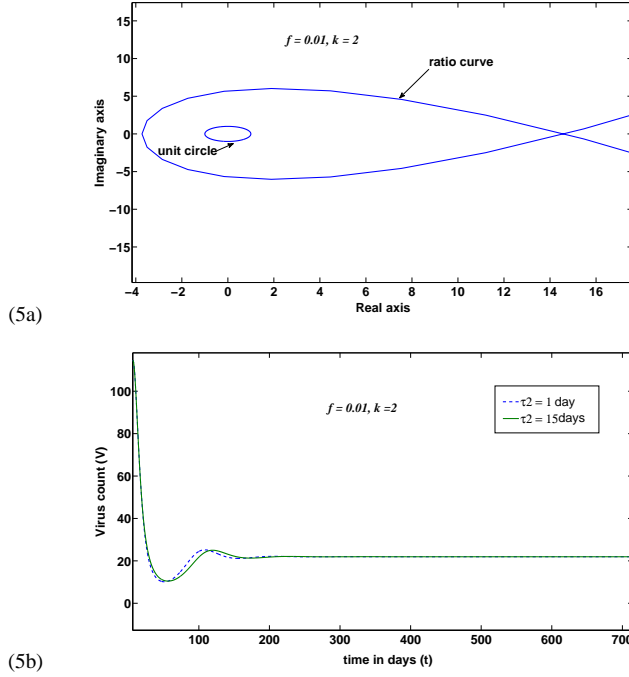


Fig. 5 Fig. 5a) Stability does not change as unit circle and ratio curve do not intersect, i.e. the equilibrium state $f = 0.01$ and $k = 2$ remains stable for $\tau_2 \neq 0$. Fig. 5b) Time series for virus particles obtained by numerical simulations for $\tau_2 \neq 0$. We see that the virus count stabilises asymptotically, i.e. the equilibrium point retains its stability.

On analysing the characteristic equation (23) we find that it is independent of τ_2 . The eigenvalues have negative real parts if $R_0 > 0$ and $f > f_c$. We can thus conclude that for $f > f_c$ only $V^* = 0$ equilibrium state exists and it is stable. It is interesting to note that for a given R_0 and $f < f_c$ there are values of $V^* \neq 0$ which may be stable or unstable as shown in Figure (2) for $\tau_2 = 0$. In that same region, $V^* = 0$ is anyway unstable. Thus, there are regions with no stable equilibrium points. The system then shows oscillatory behaviour. These regions share their boundaries with regions having stable equilibrium states. A transition from such a stable region to the completely unstable region on varying the parameter values suggests Hopf bifurcation. The richness of dynamics further increases when non-zero values of τ_2 are considered, i.e. for certain values of τ_2 the system can go from stability to instability and vice-versa.

4 Model Describing Secondary Infection

The model for secondary infection introduced here is an extension of the primary infection model given in the previous sections. Added to the primary model is a sixth variable which corresponds to the antibody formed in the previous dengue infection that still circulates in the body but is heterologous to the new virus serotype. It is observed that heterologous antibodies can bind to the virions, but the extent of binding not only depends on the com-

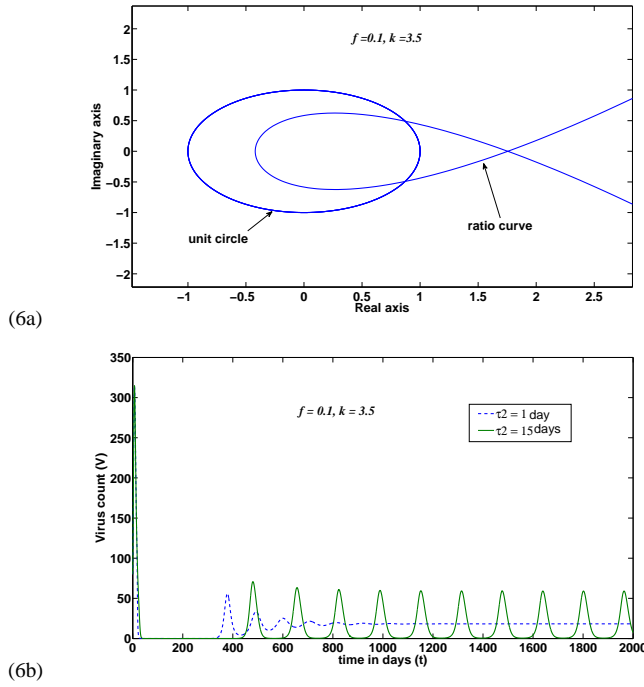


Fig. 6 Fig. 6a) Stability changes as unit circle and ratio curve intersect, i.e. the equilibrium state $f = 0.1$ and $k = 3.5$ becomes unstable for $\tau_2 \neq 0$. Fig. 6b) Time series for virus particles obtained by numerical simulations for $\tau_2 \neq 0$. We see that the virus count stabilises asymptotically for smaller values of $\tau_2 \neq 0$ but becomes oscillatory for values of τ_2 above 8.56 days. Value of τ_1 used is 10 days.

plementarity between the antigen and antibody (given in our model by the correlation factor w) but also on the concentrations of the heterologous antibodies. It is found that different serotypes of virus in the primary and secondary infections have similarities in their protein coat. As a result, the intensity with which a particular virus stimulates an antibody response for heterologous and homologous antibodies will be related. We introduce a parameter w to specifically take care of the relatedness between the various virus serotypes of primary and secondary infection. w can vary from 0 to 1 and it quantifies the similarity between the individual serotypes. For very low concentrations of the heterologous antibodies in the body, the probability of its interaction with virus particles is almost zero. At high concentrations of the heterologous antibodies there is a good probability of the virus undergoing complete opsonisation with these antibodies. In this case it is very probable that the macrophages succeed in destroying the neutralised virions. Hence at very high concentrations the heterologous antibodies actually help in curbing the infection. Thus, the mechanism of ADE is functional only between a certain concentration range of heterologous antibodies. This means when heterologous antibodies are present in the body between a certain minimum and maximum value (C_{min} and C_{max}) they actually help in virion production [23, 2]. This is incorporated in our model by introducing a dynamic switch 'y' with defined values for different ranges of antibody count. The new set of non-linear equations describing secondary dengue infection

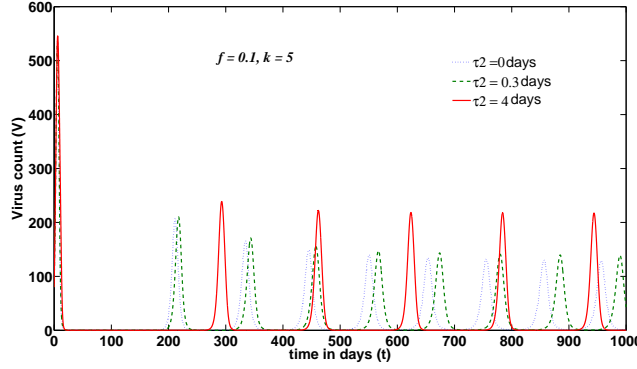


Fig. 7 Time series for virus particles with $\tau_2 \neq 0$ described by $f = 0.1$ and $k = 5$. Here we have chosen one of the τ_2 value to be 0.3 days which is close to the biological value. The same oscillatory behaviour persists for higher τ_2 values with increasing amplitude. The chosen value of τ_1 is 5 days.

are as follows:

$$\begin{aligned}
 \dot{S} &= \mu - \alpha S - aSV \\
 \dot{I} &= aSV - \beta I \\
 \dot{V} &= kI - \gamma V - yrA_1V - pA_2V \\
 \dot{B} &= \eta - \delta B + cBV \\
 \dot{A}_1 &= wfB(t - \tau_2) - qA_1V - \kappa A_1 \\
 \dot{A}_2 &= fH(t - \tau_1)B(t - \tau_2) - q'A_2V - \kappa A_2
 \end{aligned} \tag{24}$$

with,

$$\begin{aligned}
 y &= 0 & \text{for } A_1(t) \leq C_{min} \\
 y &= -1 & \text{for } C_{min} < A_1(t) \leq C_{max} \\
 y &= 1 & \text{for } A_1(t) > C_{max}
 \end{aligned} \tag{25}$$

The variable A_1 stands for the heterologous antibody previously formed on primary infection and A_2 for the homologous antibody against the new virus serotype of the secondary infection. The new parameters are, ' r '-rate at which virus particles are neutralised by A_1 antibodies and ' q '-rate at which A_2 antibody-virus complex is degraded. The Heaviside step function is not associated with the antibody A_1 as plasma cells for it are already present in the form of memory B-cells. All other parameters in this model are analogous to the primary model. An analytical study of the full 6-dimensional model becomes difficult since the parametric switch ' y ' is dynamic in nature i.e. it varies with time according to the values taken by antibody concentrations. Therefore, we try to understand the system by numerical analysis done for short and long time periods.

5 Numerical Analysis for the Secondary infection model

For a detailed numerical analysis of the secondary infection model, we simplify the model by assuming that $q = q'$ and $r = p$. Using the same parameter values as in the primary model

we numerically solve the system of equations (24) by using the 4th order Runge-Kutta method. We take $C_{max} = 500$, $C_{min} = 50$, the initial count for heterologous antibodies is determined according to the equilibrium values obtained from primary infection for same values of the relevant parameters. Here the correlation factor w is taken as 0.5 for secondary infection and 0 for primary infection.

One of the important results from the numerical analysis of our secondary infection model is that the total antibody count for secondary infection is much higher than the antibody count in the primary infection. This is shown in Figure 8). Such stronger immune response caused by higher antibody levels lead to complex and fatal manifestations resulting in DSS or DHF when infected by a different serotype of DENV [23,2,32,33,34,35]. This is also observed in patients with secondary dengue infection and we present the clinical data of the total antibody counts of primary and secondary infection from a hospital in Aurangabad, Maharashtra, India in Figure (9). Another interesting result obtained from our model is that the

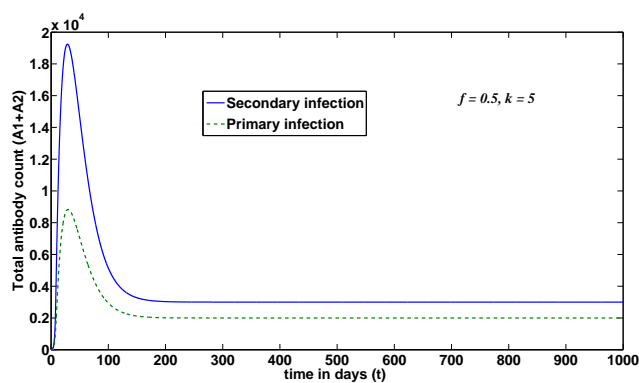


Fig. 8 Total antibody counts during primary and secondary dengue infections.

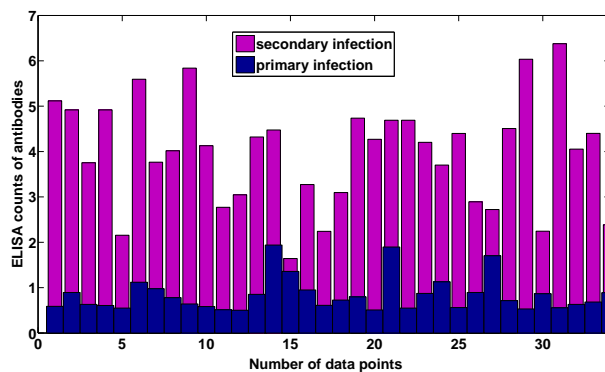


Fig. 9 Clinical data giving ELISA counts of patients during primary and secondary infections.

production of heterologous antibodies in the secondary infection enhances the production of homologous antibodies. Therefore we observe higher values of homologous antibodies in the secondary infection in comparison to homologous antibodies of the primary infection. It leads us to conclude that the higher values of total antibody counts in secondary infection are not only because of the presence of heterologous antibodies but also because of the enhancement in homologous antibody production. This result, shown in Figure (10), is in agreement with observations [23,2]. It is reported that the viral load is not detected in

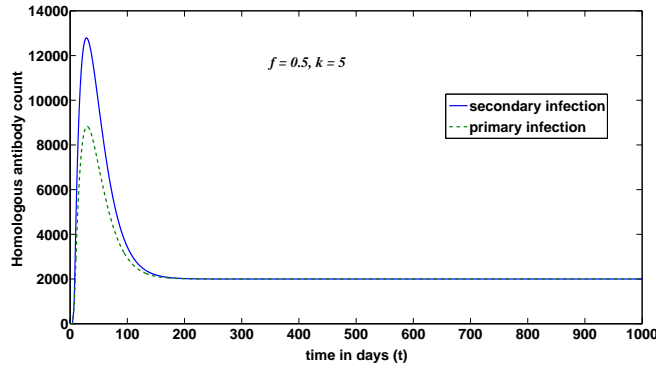


Fig. 10 Comparison of homologous antibody count in primary and secondary infections.

patients affected by secondary infection when they are suffering from severe conditions like DSS or DHF [23, 2]. Our model also indicates that the viral load clears from the body within 7 days even for secondary infection, in fact it clears faster than the primary infection. It is worth noticing that the maximum value of viral load is higher in secondary infection as compared to primary infection. This confirms that the ADE mechanism is at work. Figure (11) clearly depicts these results. Earlier studies suggest that the severity of secondary dengue

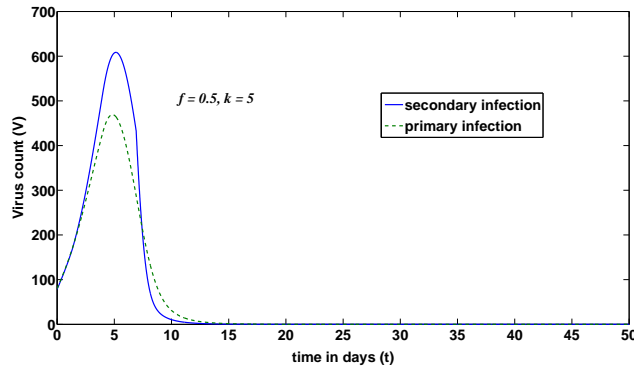


Fig. 11 Comparison of virus counts in primary and secondary infections for short time.

infection varies depending on the similarities of the two DENV serotypes involved. In our model this similarity is quantified by a measure called correlation factor w . Our results show that the enhancement of homologous antibody production in the secondary infection varies with this factor, as shown in Figure (12). Further biological studies to verify this correlation by analysing the degree of similarity between the different serotypes and the severity of infection can be done. We also identify regions of stability for the secondary infection using

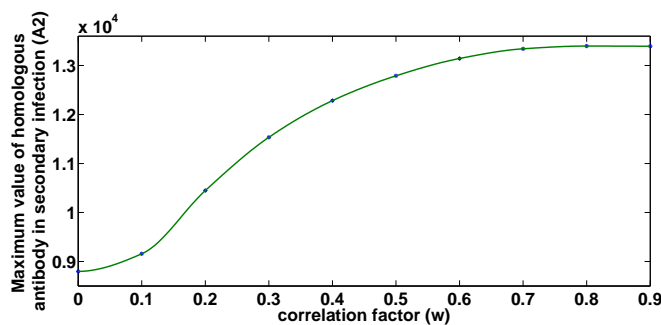


Fig. 12 Maximum homologous antibody count in secondary infection as a function of the correlation factor.

numerical simulations and show the region of stability as a function of f and k similar to that of primary infection. As the value of w increases the region of instability for non zero virus count becomes narrower as shown in the Figures(13). This implies that even though the severity of the infection might increase with w (because of enhanced antibody production) the instability region in fact decreases. Also, in the situations when the system was in the unstable region of primary infection, the outcome of the secondary infection is independent of the initial value of heterologous antibody.

6 Discussion and Conclusions

Dengue forms a major concern in the contemporary world scenario due to its severity and complexity. Considered to be a tropical disease, it is spreading to higher latitudes due to

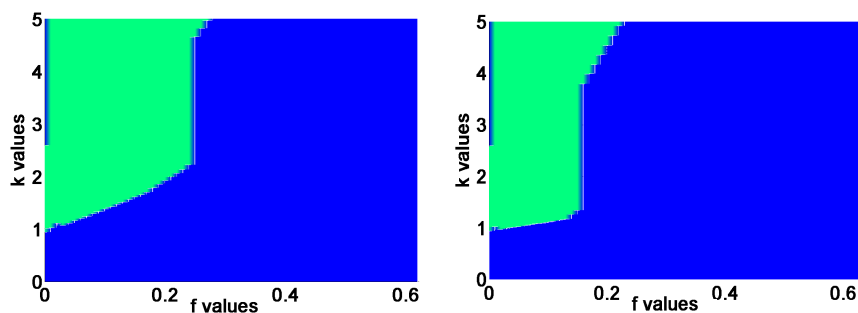


Fig. 13 Stability regions shown in blue(black) for $w = 0.5$ (left) and 0.8 (right). Green(grey) shows the unstable region.

changes in climatic and human activities. Hence, it is of great importance to study the epidemiology of dengue infections on a global macro-epidemic scale. Here we emphasise on the relevance of studying it on a micro-epidemic level to know the mechanism involved in the infection which will certainly help to eradicate it. In this paper we analyse the dynamics involved in primary infection and introduce a mathematical model describing the secondary dengue infections in accordance with the humoral immune response of the host against DENV attack. Our results show that the host immune mechanism is capable of limiting the virus growth in the early stages. The virus goes down to undetectable levels within 7-14 days as found in clinical literature. The results also imply that, in general, human body can be supposed to have a value of immune response stimulating parameter (f) higher than the critical value f_c , since, once infected, the body can easily cope with a secondary infection of the same serotype and settle to the stable region of disease free equilibrium (i.e. $V^* = 0$). The results related with the dependence of stability on time delay τ_2 are definitely interesting from an analytical point of view but it is equally interesting to see that they have any biological repercussions. Moreover, our results agree well with the observational studies of secondary infections such as a stronger immune response and a higher viral load that clears early in the infection. We have also confirmed the mechanism of ADE leading to higher viral loads. It will be interesting to experimentally verify the results related to correlation between different serotypes and their impact on the body's inflammatory response by antibody count measurements. In conclusion we note that this is the first attempt to model primary dengue infection along with the secondary infection on a micro-epidemic level using humoral immune response. We have considered delay in immune response and introduced a correlation factor and dynamic switch in the secondary infection model. The results obtained so forth are very encouraging to further extend this work for the mathematical analysis of the secondary infection model and tune it to the fine details of the unusual virus-host interactions observed in dengue infections with biological data. Further work in this direction will surely help in understanding the complex mechanisms involved in dengue pathogenesis. It will also be helpful to formulate relevant schemes to develop a dengue vaccine which can provide immunity against all four serotypes in future.

Acknowledgements We would like to thank Dr. Hedgewar Hopspital, Aurangabad, Maharashtra for providing the ELISA data on Dengue infections.

Appendix A

Details of the Jacobian and the Characteristic Equation

The Jacobian describing the primary infection in terms of V^* which is the equilibrium value virus count is given as,

$$J = \begin{bmatrix} -(\alpha + CV^*) & 0 & -\frac{\mu}{C+V^*} & 0 & 0 \\ aV^* & -\beta & \frac{\mu}{C+V^*} & 0 & 0 \\ 0 & k & -\gamma(1 + \frac{D}{C^2-V^{*2}}) & 0 & -pV^* \\ 0 & 0 & \frac{\eta}{C-V^*} & -c(C-V^*) & 0 \\ 0 & 0 & -D\gamma C^2 - V^{*2} & fe^{-\lambda\tau_2} & -q(C+V^*) \end{bmatrix} \quad (26)$$

where

$$\frac{\alpha}{a} = \frac{\delta}{c} = \frac{\kappa}{q} = C \quad (27)$$

and

$$D = \frac{fp\eta}{qc\gamma} \quad (28)$$

Let us assume

$$C + V^* = r; \quad C - V^* = s; \quad C^2 - V^{*2} = rs. \quad (29)$$

After substituting values from equations (4), the characteristic equation for the Jacobian given by (3) is:

$$\begin{aligned} G(\lambda) = & \lambda^5 + \lambda^4 \left((a+q)r + \beta + \gamma + cs + \frac{D\gamma}{rs} \right) \\ & + \lambda^3 \left((a\beta + aq + q\beta + q\gamma)r + a\gamma + \beta\gamma + acs + cs\beta + cs\gamma + cqs + \frac{D\gamma}{rs}(a + \beta) \right. \\ & \left. + D\gamma \left(\frac{c}{r} + \frac{q}{s}(r-s) \frac{Dp\gamma}{2rs} + \frac{k\mu}{r} \right) \right) \\ & + \lambda^2 \left((ar\beta\gamma + cs\beta\gamma + qr\beta\gamma + cqs\gamma + acsr\gamma + aq\gamma r^2) \left(1 + \frac{D}{rs} \right) + acsr\beta r + aq\beta r^2 \right. \\ & + acqsr^2 + cqs\beta r(ar + \beta + cs)pD\gamma \frac{(r-s)}{2rs} + k\mu \frac{(ar + cs + qs)}{r} - ak\mu \frac{(r-s)}{2r} \\ & + \lambda \left((acrs\beta\gamma + aq\beta\gamma r^2 + cqs\beta\gamma + acqsr^2) \left(1 + \frac{D}{rs} \right) + acqsr^2 \right. \\ & - pD\gamma(r-s) \frac{(ar\beta + cs\beta + arcs)}{2rs} + k\mu(acr + aqr + csq) - ak\mu(r-s) \frac{(cs + qr)}{2r} \\ & + (aqcs\beta\gamma r^2 \left(1 + \frac{D}{rs} \right) - acpD\beta\gamma \frac{(r-s)}{2} + akcqs\mu r - akcqs\mu \frac{(r-s)}{2}) \\ & \left. + e^{-\lambda\tau_2} \left(\lambda^2 (fp\eta \frac{(r-s)}{2r}) + \lambda (fp\eta(ar + \beta) \frac{(r-s)}{2s}) + fpar\eta\beta \frac{(r-s)}{2s} \right) \right) = 0 \end{aligned} \quad (30)$$

We can now rewrite the characteristic equation as:

$$G(\lambda) = \lambda^5 + G_4\lambda^4 + G_3\lambda^3 + G_2\lambda^2 + G_1\lambda^1 + G_0\lambda + H_2e^{-\lambda\tau_2}\lambda^2 + H_1e^{-\lambda\tau_2}\lambda + H_0e^{-\lambda\tau_2} = 0 \quad (31)$$

Where:

$$\begin{aligned}
G_4 &= ((a+q)r + \beta + \gamma + cs + \frac{D\gamma}{rs}); \\
G_3 &= ((a\beta + aq + q\beta + q\gamma)r + a\gamma + \gamma\beta + acs + cs\gamma + cs\beta + cqs + \\
&+ \gamma\frac{D}{rs}(a + \beta) + D\gamma(\frac{c}{r} + \frac{q}{s})pD\gamma\frac{(r-s)}{2rs} + \frac{k\mu}{r}); \quad (32) \\
G_2 &= ((ar\beta\gamma + cs\beta\gamma + qr\beta\gamma + srcq\gamma + acsr\gamma + aq\gamma r^2)(1 + \frac{D}{rs}) + acsr\beta + aq\beta r^2 + acqsr^2 \\
&+ cqs\beta - (ar + \beta + cs)pD\gamma\frac{(r-s)}{2rs} + k\mu\frac{(ar + cs + qs)}{r} - ak\mu\frac{(r-s)}{2r}); \\
G_1 &= ((acrs\beta\gamma + aq\beta\gamma r^2 + cqs\beta\gamma + acqsr^2)(1 + \frac{D}{rs}) + acqs\beta r^2 \\
&- pD\gamma(r-s)\frac{(ar\beta + cs\beta + arcs)}{2rs} + k\mu(ac + aqr + csq) - ak\mu(r-s)\frac{(cs + qr)}{2r}); \\
G_0 &= (aqcs\beta\gamma r^2(1 + \frac{D}{rs}) - acpD\beta\gamma\frac{(r-s)}{2} + akcqs\mu r - akcqs\mu\frac{(r-s)}{2}); \\
H_2 &= (fp\eta\frac{(r-s)}{2r}); \\
H_1 &= (fp\eta(ar + \beta)\frac{(r-s)}{2s}); \\
H_0 &= afpr\eta\beta\frac{(r-s)}{2s} \quad ; \quad (33)
\end{aligned}$$

We carry out further analysis in the paper by considering the coefficient values given above.

References

1. Lindenbach D, Rice CM, Flaviviridae: the Viruses and their Replication. In: Knipe DM, Howley PM, Griffin DE, Lamb RA, Malcolm AM, Roizman B, Straus SE (eds), Fields Virology, Lippincott Williams & Wilkins, Philadelphia, 991-1041, (2001)
2. Halstead SB, Pathogenesis of Dengue: Challenges to Molecular Biology, Science, 239, 476-481 (1988)
3. Gibbons RV, Vaughn DW, Dengue: an Escalating Problem, BMJ, 324, 1563-1566 (2002)
4. Halstead SB, Dengue, Lancet, 370, 1644-1652 (2007).
5. Rigau-Perez JG, Clark GG, Gubler DJ, Reiter P, Sanders EJ, Vorndam AV, Dengue and Dengue Haemorrhagic Fever, Lancet, 352, 971-977 (1998).
6. Dietz K, Transmission and control of arbovirus diseases. In: Epidemiology, Ludwig D, Cooke KL, (eds), Philadelphia, PA: Society for Industrial and Applied Mathematics, 104-121 (1975)
7. Esteva L, Vargas C, Analysis of a Dengue Disease Transmission Model, Math. Biosci., 15, 131-151 (1998)
8. Esteva L, Vargas C, A Model for Dengue Disease with Variable Human Population, J. Math. Biol., 38, 220-240 (1999)
9. Esteva L, Vargas C, Coexistence of Different Serotypes of Dengue Virus, J. Math. Biol., 46, 31-47 (2003)
10. Feng Z, Velasco-Hernandez JK, Competitive Exclusion in Vector Host-Model for the Dengue Fever, J. Math. Biol., 35, 523-544 (1997)
11. Derouich M, Boutayeb A, Dengue Fever: Mathematical Modelling and Computer Simulation, Applied Mathematics and Computation, 177, 528-544 (2006)
12. Garba SM, Gumel AB, Abu Bakar MR, Backward Bifurcations in Dengue Transmission Dynamics, Mathematical Biosciences, 215, 1125 (2008)
13. Nuraini N, Soewono E, Sidarto KA, A Mathematical Model of Dengue Internal Transmission Process, J. Indones. Math. Soc. (MIHMI), 13-1, 123-132 (2007)
14. Nowak MA, May RM, Virus Dynamics: Mathematical Principles of Immunology and Virology, Oxford University Press (2000)

15. Ambika G, Dahanukar N, Virus Immune Drug Dynamics, In: Nonlinear Dynamics, Daniel M, Rajasekar S. (eds), Narosa Publication, India, (2009)
16. Nuraini N, Tasman H, Soewono E, Sidarto KA, A with-in host Dengue infection model with immune response, Mathematical and Computer Modelling, 49, 1148-1155, (2009)
17. Chaturvedi UC, Tandon Pushpa, Mathur Asha, Kumar A, Host Defence Mechanisms Against Dengue Virus Infection of Mice, J. Gen. Virol., 39, 293-302 (1978)
18. Run Tao He, Innis BL, Nisalak A, Usawattanakul W, Wang S, Kalayanaroj S, Anderson R, Antibodies that block virus attachment to vero cells are a major component of the human neutralizing antibody response against dengue virus type 2, J. Med. Virol, 45, 451-461 (1995)
19. Jindadamrongwech S, Thepparit C, Smith DR, Identification of GRP 78 (BiP) as a liver cell expressed receptor element for dengue virus serotype 2, Arch Virol, 149, 915-927 (2004)
20. Kliks SC, Nisalak A, Brandt WE, Wahl L, Burke DS, Antibody - dependent enhancement of dengue virus growth in human monocytes as a risk factor for dengue hemorrhagic fever, Am. J. Trop. Med. Hyg., 40, 444-451 (1989)
21. Tassaneetrithep B, Burgess TH, Granelli-Piperno A, Trumpfheller C, Finke J, Sun W, Eller MA, Pattanapanyasat K, Sarasombath S, et al, DC SIGN (CD209) mediates dengue virus infection of human dendritic cells, J. Exp. Med., 197, 823-829 (2003)
22. Wu SJ, Grouard-Vogel G, Sun W, Mascola JR, Brachtel E, Putvatana R, Louder MK, Filgueira L, Marovich MA, Wong HK, Blauvelt A, Murphy GS, Robb ML, Innes BL, Bix DL, Hayes CG and Frankel SS, Human skin Langerhans cells are targets of dengue virus infection, Nat. Med., 6, 816-820 (2000)
23. Halstead SB, Observations Related to Pathogenesis of Dengue Hemorrhagic Fever VI. Hypothesis and Discussion, Yale Journal of Biology and Medicine, 42, 350-362 (1970)
24. Dibrov BF, Livshits MA, Volkenstein MV, Mathematical model of immune processes, J. Theor. Biol., 65, 609-631 (1977a)
25. Fowler AC, Approximate Solution of a Model of Biological Immune Responses Incorporating Delay, J. Math. Biology, 13, 23-45 (1981)
26. Janeway Jr CA, Travers P, Walport M, et al, Immunobiology: The Immune System in Health and Disease, 5th edition, Garland Science, New York (2001)
27. Diekmann O, Heesterbeek JAP, Mathematical Epidemiology of Infectious Diseases, Model Building, Analysis and Interpretation, John Wiley & Sons, Chichester (2000).
28. Leenheer PD, Smith HL, Virus Dynamics: A Global Analysis, SIAM J. Appl. Math., 63, 1313-1327, (2003)
29. Strogatz SH, Non linear Dynamics and Chaos Perseus Books, Reading, Massachusetts (1994) .
30. Lakshmanan M, Senthilkumar DV Dynamics of Non-linear Time Delay Systems, Springer-Verlag Berlin Heidelberg (2010).
31. Koscielnaik S, Analytic Criteria for Stability of Beam Loaded Radio Frequency Systems, Particle Accelerators, 48, 135-168 (1994).
32. Fink J, Gu F, Vasudevan SG, Role of T cells, Cytokines and Antibody in Dengue Fever and Dengue Haemorrhagic Fever, Rev. Med. Virol., 16, 263-275 (2006).
33. Lei HY, Yeh TM, Liu HS, Lin YS, Chen SH, Liu C, Immunopathogenesis of Dengue Virus Infection, J. Biomed. Sci., 8, 377-388 (2001)
34. Rothman AL, Ennis FA, Immunopathogenesis of Dengue hemorrhagic fever, Virology, 257, 1-6 (1999)
35. Rothman AL, Dengue: defining protective versus pathologic immunity, J. Clin. Invest., 113, 946-951 (2004)